Supporting Online Material

Materials and Methods

Av1 and Av2 were isolated and purified under anaerobic conditions according to published protocols (*S1*). Crystals of nf-, pcp- and adp-Av2:Av1 complexes were prepared in sitting drops by vapor diffusion in an anaerobic chamber at room temperature. All solutions and chemicals used for crystallization were thoroughly deaerated using vacuum/Ar-fill cycles. Precipitating solutions for the nf-complex contained 16-18% (w/v) PEG 10000, and those for pcp- and adp- complexes contained 18-22% PEG 8000 (w/v), in addition to 0-50 mM NaCl, 100 mM Tris buffer (pH 8.5), and 10 mM dithionite. The protein solutions were prepared by mixing appropriate amounts of Av1 and Av2 stock solutions ($[Av1]_{stock}$= ~20 mg/ml, $[Av2]_{stock}$= ~40 mg/ml), both of which were in 100 mM Tris (pH 7.75), 200 mM NaCl and 5 mM dithionite. Best crystals for nf-, pcp- and adp-complexes were obtained using 1:1.2 to 1:1.5 Av1:Av2 ratios (v/v), corresponding to 5 to 6-fold molar excess of Av2 over per active site of Av1. The protein solutions for pcp- and adp-complexes also contained 10 mM $MgCl_2$ (added from a 1 M stock), and 10 mM AMPPCP or ADP, whose 100 mM stock solutions were prepared in 100 mM Tris buffer (pH 8.5) immediately prior to setting up the crystallization trays. The crystallization drops contained 2 μl of the precipitating solution and 2 μl of the protein mixture, and the reservoir contained 250 μl of the precipitating solution. Brown, rod-shaped crystals appeared after 2-3 days and reached full growth after 1-2 weeks. The crystals for nf- and pcp-complexes were orthorhombic ($P2_12_12_1$), and those for the adp-complex were triclinic (P1) (see Table S1 for unit cell dimensions).

For data collection, suitable crystals were exchanged into 25% PEG 400 over five steps in one hour for cryoprotection and flash-frozen in liquid nitrogen. X-ray diffraction data for the nf-complex were collected at SSRL (BL 9-1) and those for pcp- and adp-complexes were acquired at ALS (BL 8.2.1) on ADSC CCD detectors using x-rays of wavelengths 0.9796 Å, 1.000 Å, and 1.000 Å, respectively. Data collection and refinement statistics are summarized in Table S1. Data sets were processed using DENZO-SCALEPACK (*S2*) for nf- and adp-complexes and MOSFLM (*S3*)-SCALA (*S4*) for the pcp-complex. The initial phases were obtained by molecular replacement using MOLREP (*S4*) with Av1 (PDB code: 1M1N) as a model. Initial electron density maps clearly revealed the positions of the iron-sulfur clusters and most secondary structure elements of Av2 molecules, allowing their manual placement using native Av2 (PDB code: 1G5P) and ADP•AlF_4^- complexed Av2 (PDB code: 1M34) as models.

After an initial round of rigid-body refinement with CNS (*S5*) and manual rebuilding with MAIN (*S6*), simulated annealing using Ramachandran potentials and a very low X-ray weight was performed to regularize geometry. Ramachandran potentials were utilized during refinement of the adp-Av2:Av1 structure. In the absence of such potentials, the refinement was less well-behaved as evidenced by high free R-factors (>33%). Simulated-annealing, positional and thermal refinement with CNS, along with manual rebuilding and water placement with XFIT (*S7*) and MAIN (*S6*) produced the final models. In case of the adp-complex, eight-fold cyclic NCS-averaging of the individual α-subunits of the four Av2 molecules in the asymmetric unit (using MAIN), in combination with 4-fold averaging of the individual Av1 $\alpha\beta$-dimers produced higher quality maps in the regions where the four Av2 molecules were structurally similar. The

averaged maps were used along with the non-averaged maps as a guide for manual rebuilding. Bulk solvent correction and anisotropic B-factor scaling were applied to the reflection data. NCS restraints (300 kcal mol^{-1} $Å^{-2}$) were applied to four equivalent Av1 $\alpha\beta$-dimers and kept throughout the refinement. The stereochemistry of the final models was calculated using PROCHECK (*S8*). Final refinement statistics are indicated in Table S1. A listing of all residues included in the final model is provided in Table S3, with an evaluation of the quality of electron density for backbone and sidechain atoms. Figures were prepared using PYMOL (*S9*), MOLSCRIPT (*S10*) and RASTER3D (*S11*). The coordinates of the nf-Av2:Av1, pcp-Av2:Av1 and adp-Av2:Av1 complexes will be deposited in the Protein Data Bank (www.rcsb.org/pdb) for release upon publication.

S1. D. Wolle, C. H. Kim, D. Dean, J. B. Howard, *J. Biol. Chem.* **267**, 3667 (1992).

S2. Z. Otwinowski, W. Minor, in *Macromolecular Crystallography, Part A.* (1997), vol. 276, pp. 307-326.

S3. A. G. W. Leslie, MOSFLM v6.2.0, Cambridge, U.K. (2003)

S4. CCP4, *Acta Crystallogr. Sect. D Biol. Crystallogr.* **50** (1994).

S5. A. T. Brünger *et al.*, *Acta Crystallogr. D* **54**, 905 (1998).

S6. D. Turk, in *Proceedings from the 1996 Meeting of the International Union of Crystallography Macromolecular Computing School* P. E. Bourne, K. Watenpaugh, Eds. (1996).

S7. D. E. McRee, *J. Mol. Graphics* **10**, 44 (1992).

S8. R. A. Laskowski, M. W. Macarthur, D. S. Moss, J. M. Thornton, *J. Appl. Crystallogr.* **26**, 283 (1993).

S9. W. L. DeLano, *The PYMOL Molecular Graphics System (http://www.pymol.org)* (2003).

S10. P. J. Kraulis, *J. Appl. Cryst.* **24**, 946 (1991).

S11. E. A. Merritt, M. E. P. Murphy, *Acta Crystallogr. D* **50**, 869 (1994).

Table S1. Data collection and refinement statistics.

	nf-Av2:Av1	**pcp-Av2:Av1**	**adp-Av2:Av1**
Data Collection			
Space group	$P2_12_12_1$	$P2_12_12_1$	P1
Cell dimensions			
a, b, c (Å)	170.9, 75.9 , 223.7	110.5, 120.9, 264.8	72.9, 141.4, 165.5
α, β, γ(°)	90, 90, 90	90, 90, 90	73.7 , 79.4 , 76.6
Resolution (Å)	50.0 – 2.1	50.0 – 2.3	50.0 – 3.1
No. of total observations	578,292	583,968	169,772
Redundancy	3.6	3.4	1.7
R_{symm} (%)[a,b]	14.0 (53.6)	12.3 (37.8)	7.5 (24.2)
$I/\sigma(I)$[a]	8.7 (2.5)	12.0 (3.4)	8.8 (2.7)
Completeness (%)[a]	95.7 (89.5)	89.2 (85.7)	88.2 (72.0)
Refinement			
Resolution (Å)	43.0 - 2.1	50.0 – 2.3	50.0 – 3.1
R (%)[a,c]	17.2	23.5	22.9
R_{free} (%)[a,d]	22.1	27.5	27.0
R.m.s. deviations from ideal values			
bond lengths (Å)	0.013	0.015	0.015
bond angles (°)	2.3	2.4	2.6
Ramachandran statistics			
most favored (%)	88.2	92.2	95.2
additionally allowed (%)	11.4	7.4	4.7
generously allowed (%)	0.4	0.4	0.1
disallowed (%)	0.0	0.0	0.0

[a] Values in parentheses correspond to the highest resolution shell.
[b] $R_{symm} = \sum_{hkl,i}(\sum_i |I_{hkl,i} - \langle I_{hkl}\rangle|)/\sum_{hkl,i}\langle I_{hkl}\rangle$, where $I_{hkl,i}$ is the scaled intensity of the ith individual measurement of the reflection with indices *hkl*, and $\langle I_{hkl}\rangle$ is the mean intensity of that reflection.
[c] $R = \sum\sum |F_{obs}| - |F_{calc}|| / \sum\sum |F_{obs}|$ for all reflections (no σ cutoff).
[d] Free R calculated against 5% (nf), 7% (pcp) and 10% (adp) of the reflections randomly removed.
[e] Ramachandran potentials were applied throughout the refinement for the adp:Av2-Av1 complex.

Table S2 Residues included in the final structural models for the nf-Av2:Av1, pcp-Av2:Av1 and adp-Av2:Av1 complexes. Residues with observable electron density for backbone atoms are included in the structural models; residues with poorly defined sidechain electron density are also included, but with the occupancy set to zero. Chains ABCD and IJKL correspond to the subunits of crystallographically distinct Av1 tetramers, while EF, GH, MN and OP are the subunits of crystallographically distinct Av2 dimers.

nf-Av1:Av2

Chain	Backbone defined	Residues with poor sidechain density
A	5-480	212, 332
B	2-523	
C	4-480	
D	2-523	
E	1-289	
F	1-286	

pcp-Av1:Av2

Chain	Backbone defined	Residues with poor sidechain density
A	4-480	
B	2-523	
C	5-480	
D	2-523	26, 258
E	1-50, 54-270	71, 74, 84, 92, 116-117, 127, 154, 159, 166, 170-171, 190-191, 194, 202, 211, 223-224, 233, 235, 262
F	1-50, 54-263	68, 80, 111, 116-118, 155, 163, 190-191, 233, 235, 257, 261
G	1-51, 54-272	54, 69, 74, 77, 116, 159, 186, 215, 221, 223-224, 230, 233, 235, 245
H	1-262	52, 54, 77, 118, 129, 155, 262

adp-Av1:Av2

Chain	Backbone defined	Residues with poor sidechain density
A	5-480	23, 30, 50-51, 101, 129, 168
B	2-523	143, 171, 177-178, 211, 303, 400, 417
C	5-480	7, 30, 43, 68, 70, 288
D	2-523	120, 171
E	2-88, 90-126, 129-157, 159-180, 182-191, 203-234, 237-271	10, 32, 39, 41, 46, 56, 58-60, 63, 72-74, 77, 84, 87, 100, 102, 109, 116, 119-121, 130, 135, 137, 140-141, 143, 154, 166, 171, 173-174, 179, 183, 185, 187-189, 191, 206, 211, 213-216, 219, 223, 230-231, 233, 239-240, 245-246, 249-251, 263-266, 270
F	1-62, 67-228, 230-275	8, 32, 46, 48-49, 52, 58, 60, 67-68, 70, 72-73, 77, 84, 92, 107, 110, 116, 127, 129, 137, 140-141, 143, 146, 166, 170-171, 187, 190, 194, 199, 202, 219, 221, 223-224, 230-231, 245, 251, 261
G	1-89, 93-94, 98-263	10, 15, 28, 31-32, 41, 46, 52, 54-56, 59, 68, 71, 75-77, 84, 100, 103-104, 108, 116, 118, 127, 135, 140, 155, 179, 182, 187-188, 191-192, 194-195, 202, 213, 223-224, 229, 235, 245-246, 249, 251-252, 262
H	2-7, 10-41, 81-88, 92-104, 119-155, 157-169, 175-185, 193-202, 205-219, 240-250, 255-258, 261-270	10, 15, 18, 20-21, 23, 26, 28-29, 31-32, 39, 41, 84, 87, 92, 100, 102-103, 121, 127, 137, 140, 142-143, 146, 154-155, 158-159, 163, 166, 169, 178, 182, 184-185, 194-195, 202, 210, 217-219, 241, 245-246, 250, 255, 257, 261, 263, 266, 269
I	5-480	
J	2-523	
K	5-480	125, 129, 133
L	2-523	
M	4-49, 52-69, 71-76, 78-88, 91-95, 97-120, 123-142, 144-183, 185-186, 191-271	4, 10, 15, 21, 29, 31-32, 39, 41, 43, 46-47, 52, 54-55, 60, 66-68, 71-72, 74-76, 84, 92, 100, 111, 116, 119, 135, 146, 151, 154-156, 158-159, 166, 170, 178, 182, 191-194, 199, 202-203, 207, 210, 213-219, 221, 224, 235, 241, 245, 251-252, 259-261, 264-265, 269, 271
N	4-22, 33-36, 40-44, 81-86, 96-117, 121-132, 137-143, 150, 156-170, 182-183, 193-204, 208-213,	4, 8, 10, 18, 20, 22, 33-36, 41, 84, 100, 102-104, 106-112, 115-116, 121, 123-124, 137, 139-140, 142-143, 156, 158-159, 166, 170, 182-183, 194-195, 199, 201-203, 208-210, 213, 216, 218-219, 221, 223-224, 239-241, 243, 245-248, 251-253, 255-256, 262-263, 265-268, 270

Chain	Backbone defined	Residues with poor sidechain density
	216-225, 227-228, 237-257, 261-273	
O	2-114, 117-263	10, 22, 26, 29, 31-33, 40, 46, 52, 57, 67-68, 74, 76-77, 84, 100, 108, 111, 117-119, 129-131, 141, 146, 165-166, 168-170, 182, 187, 191, 194, 202-203, 213, 217, 219, 221, 223-228, 235-236, 238, 241, 245-246, 249, 251-254, 262
P	6-20, 22-31, 36-39, 54-61, 80-82, 87-117, 123-142, 144-170, 180-184, 193-212, 214-220, 223-236, 239-252, 261-272	10, 15, 31, 58-60, 80, 92, 111-112, 115, 117, 123, 130, 139-141, 145-148, 154, 163, 165, 170, 194, 196, 202-203, 205, 208, 210, 218-219, 223-224, 229, 233, 235, 239-241, 243, 246, 249-251, 261, 263-266, 269, 271

Table S3 Pairwise comparisons of different Fe-protein conformations

structure	native Av2	Av2 + ADP	alf-Av2	ΔLeu-β127	ΔLeu-β127+ ATP	nf-Av2	pcp-Av2		adp-Av2		
native Av2 (1G5P)											
β											
Av2 + ADP (1FP6)	1.3										
β	0.7										
alf-Av2 (1M34)	3.9	3.0									
β	1.5	1.2									
ΔLeu-β127 Av2 (1G20)	3.4	2.5	1.5								
β	1.4	1.3	0.8								
ΔLeu-β127 Av2 + ATP (1G21)	2.9	2.0	1.7	1.1							
β	1.4	1.2	0.5	0.8							
nf-Av2 (chains EF)	1.0	1.5	4.0	3.5	2.9						
β	0.8	0.9	1.5	1.4	1.4						
pcp-Av2 (chains EF)	3.5	2.6	1.7	1.2	0.9	3.4					
β	1.6	1.4	0.7	1.0	0.8	1.6					
pcp-Av2 (chains GH)	3.1	2.1	1.6	1.1	0.6	3.0	0.8				
β	1.4	1.2	0.4	0.8	0.5	1.5	0.6				
adp1-Av2 (chains EF)	1.4	0.7	2.9	2.5	2.1	1.6	2.6	2.2			
β	0.7	0.6	1.3	1.3	1.2	0.8	1.4	1.2			
adp2-Av2 (chains GH)	1.3	0.7	3.1	2.5	2.1	1.4	2.6	2.2	0.6		
β	0.7	0.6	1.3	1.3	1.2	0.8	1.4	1.3	0.3		
adp3-Av2 (chains MN)	1.0	1.5	3.8	3.5	3.0	1.3	3.5	3.2	1.4	1.3	
β	0.7	0.6	1.3	1.3	1.2	0.8	1.4	1.3	0.3	0.3	
adp4-Av2 (chains OP)	1.2	0.7	3.3	2.6	2.2	1.3	2.7	2.3	0.7	0.5	1.4
β	0.7	0.6	1.3	1.2	1.2	0.8	1.4	1.2	0.3	0.3	0.3

Table S3 Root mean square deviations (in Å) between pairs of superimposed Fe-protein structures. The first five structures and their PDB IDs (in parentheses) have been previously deposited and serve as reference structures. When multiple Fe-protein dimers were present in the asymmetric unit of a reference structure, the first set of subunits was used. The remaining seven structures have been determined in the course of this work; the chain labels for the specified dimer are in parentheses. The Cα's of 236 residues (6-49, 56-115, 120-125, 129-186 and 193-260) present in each subunit of all available Fe-protein models were used for the comparison. The first line in each entry corresponds to the superposition of both subunits in each dimer; for example, subunits AB of one dimer are superimposed onto EF of the other (but subunits AB are not superimposed onto subunits FE). The second line corresponds to the superposition of individual subunits, calculated as the average of the A-E, A-F, B-E and B-F comparisons. The entries outlined in dark boxes designate the closest comparisons between the reference structures and the complexes determined in this work; specifically, the nf-Av2 structure most closely resembles native Av2; the pcp-Av2 structure most closely resembles the ΔLeu-α127+ATP structure; three of the adp-Av2 dimers (adp1, adp2 and adp4) most closely resemble the ADP bound state of Av2 in the absence of MoFe-protein, while the adp3 most closely resembles native Av2. In all cases, the best superpositions exhibit root mean square deviations for both the dimer and individual subunit comparisons $\leq$ 1 Å.

Table S4 Intermolecular polar interactions in the nitrogenase complexes. Contacts between oxygen and/or nitrogen atoms in the indicated Fe-protein - MoFe-protein complexes were identified with the CCP4 program CONTACT (*S4*) using a cutoff of 3.4 Å. "mc" indicates that the contact involves the main chain atoms of a specified residue; otherwise, the contacts are mediated by side chain groups. α_1- and α_2- designate the Fe-protein subunits in a given dimer that interact most closely with the α- and β-subunits of the MoFe-protein, respectively. "*" designates poor electron density for the designated side chain so that reliable placement could not be established; these residues are included to identify the interaction region. Due to disordering of the Fe-protein subunits, side chain density was weak for the adp3-Av2 and adp4-Av2 molecules. Contacts in the alf-Av2:Av1 structure (PDB ID 1M34) are included for comparison to the pcp-Av2:Av1 complex.

Table S4 cont'd

pcp-Av2:Av1 intermolecular contacts					
Av1 residue		mc	Av2 residue		mc
Lys	51*		Gly	α_1-65	mc
Glu	120		Arg	α_2-100	
Glu	120		Thr	α_2-104	
Ile	123	mc	Cys	α_2-97	mc
Val	124	mc	Cys	α_2-97	mc
Gly	157	mc	Arg	α_1-100	
Ile	159	mc	Gly	α_1-133	mc
Gly	160	mc	Arg	α_1-140	
Asp	161	mc	Arg	α_1-140	
Glu	184		Arg	α_1-100	
Glu	120		Arg	α_1-100	
Glu	120		Thr	α_1-104	
Asp	121		Gly	α_1-65	mc
Val	124	mc	Cys	α_1-97	mc
Glu	156	mc	Arg	α_2-100	
Ile	158	mc	Gly	α_2-133	mc
Asn	163		Glu	α_2-141	
Asn	167		Ser	α_2-174	mc
Asn	168		Lys	α_2-170	mc

alf-Av2:Av1 (PDB ID 1M34) intermolecular contacts					
Av1 residue		mc	Av2 residue		mc
Lys	51		Gly	α_1-65	mc
Glu	120		Arg	α_2-100	
Glu	120		Thr	α_2-104	
Ile	123	mc	Cys	α_2-97	mc
Val	124	mc	Cys	α_2-97	mc
Asp	128		Lys	α_1-170	
Gly	157	mc	Arg	α_1-100	
Ile	159	mc	Gly	α_1-133	mc
Gly	160	mc	Arg	α_1-140	
Asp	161	mc	Arg	α_1-140	
Ser	165		Ser	α_1-174	
Lys	168		Glu	α_1-141	
Arg	182		Arg	α_1-140	
Glu	184		Arg	α_1-100	
Glu	120		Arg	α_1-100	
Glu	120		Thr	α_1-104	
Ala	123	mc	Cys	α_1-97	mc
Val	124	mc	Cys	α_1-97	mc
Glu	156		Arg	α_2-100	
Ile	158	mc	Gly	α_2-133	mc
Gly	159	mc	Arg	α_2-140	
Asp	160	mc	Arg	α_2-140	
Asp	161	mc	Arg	α_2-140	
Asn	163		Glu	α_2-141	
Asn	167		Glu	α_2-141	
Asn	167		Ser	α_2-174	mc
Asn	168		Lys	α_2-170	mc
Lys	171		Asn	α_2-173	mc
Lys	400		Asp	α_2-69	

Table S4 cont'd

nf-Av2:Av1 intermolecular contacts					
Av1 residue		mc	Av2 residue		mc
Glu	120		Asn	$_2$-107	
Lys	121		Ala	$_2$-61	mc
Lys	121		Ala	$_2$-64	mc
Lys	121		Thr	$_2$-66	mc
Gly	160	mc	Arg	$_1$-140	
Glu	156	mc	Arg	$_2$-100	
Val	157	mc	Arg	$_1$-100*	
Ile	158	mc	Arg	$_1$-100*	
Asp	161		Tyr	$_2$-171	
Asn	163		Lys	$_2$-170	mc
Asn	163		Asn	$_2$-173	
Lys	211		Ala	$_2$-172	mc
Lys	211		Gly	$_2$-175	mc
Lys	211		Arg	$_2$-178	
Asn	399		Glu	$_2$-111*	
Lys	400		Glu	$_2$-68	mc
Lys	400		Leu	$_2$-70	mc
Lys	400		Glu	$_2$-112	
Arg	401		Glu	$_2$-111	mc

adp-Av2:Av1 intermolecular contacts					
Av1 residue		mc	Av2 residue		mc
adp1 (chains ABEF)					
Lys	50*		Glu	$_1$-68*	
Val	124	mc	Arg	$_2$-100	
Phe	125	mc	Arg	$_2$-100	
Gly	157	mc	Arg	$_1$-100*	
Ile	159	mc	Arg	$_2$-100	
Asp	162		Arg	$_1$-140*	
Asp	121		Gly	$_1$-65	mc
Asp	121		Val	$_1$-67	mc
adp2 (chains CDGH)					
Lys	50		Glu	$_1$-68*	
Lys	168		Asn	$_1$-173	mc
Val	157	mc	Arg	$_2$-100*	
adp3* (chains IJMN)					
Ile	159	mc	Arg	$_2$-100	
Gly	160	mc	Arg	$_2$-100	
adp4* (chains KLOP)					
Lys	26		Asp	$_1$-69	
Lys	30		Asp	$_1$-69	
Lys	50		Glu	$_1$-68	
Lys	50		Glu	$_1$-111	
Leu	158	mc	Arg	$_2$-100	
Asp	162		Lys	$_1$-170	
Ser	165		Lys	$_1$-170	
Lys	168		Asn	$_1$-173	
Glu	120	mc	Arg	$_1$-100	

Table S5. Parameters describing Av2 – Av1 docking interactions for the individual adp-conformers. adp1-Av2, adp2-Av2, adp3-Av2 and adp4-Av2 designate specific Fe-protein dimers in the adp-Av2:Av1 structure with Av2 chain identifiers EF, GH, MN and OP, that are associated with Av1 subunits AB, CD, IJ and KL, respectively.

complex	Buried surface area ($Å^2$)	β-100 helix-helix angle β (°)	[4Fe:4S] – P-cluster distance (Å)
adp1-Av2	2000	26	22.6
adp2-Av2	1700	29	22.8
adp3 -Av2	1600	31	23.8
adp4 -Av2	1900	33	23.7

Supplementary Figure Legends

Fig. S1. Docking geometries and protein-protein interaction surfaces in (A) adp1- Av2:Av1, (B) adp2- Av2:Av1, and (C) adp3- Av2:Av1.

Fig. S2. Crosslinking region in nf-Av2:Av1, illustrating the H-bonding network involving Lys-β400, Glu-β112, Glu-β68 and Glu-β70. The $2F_o - F_c$ map (purple) is contoured at 1σ.

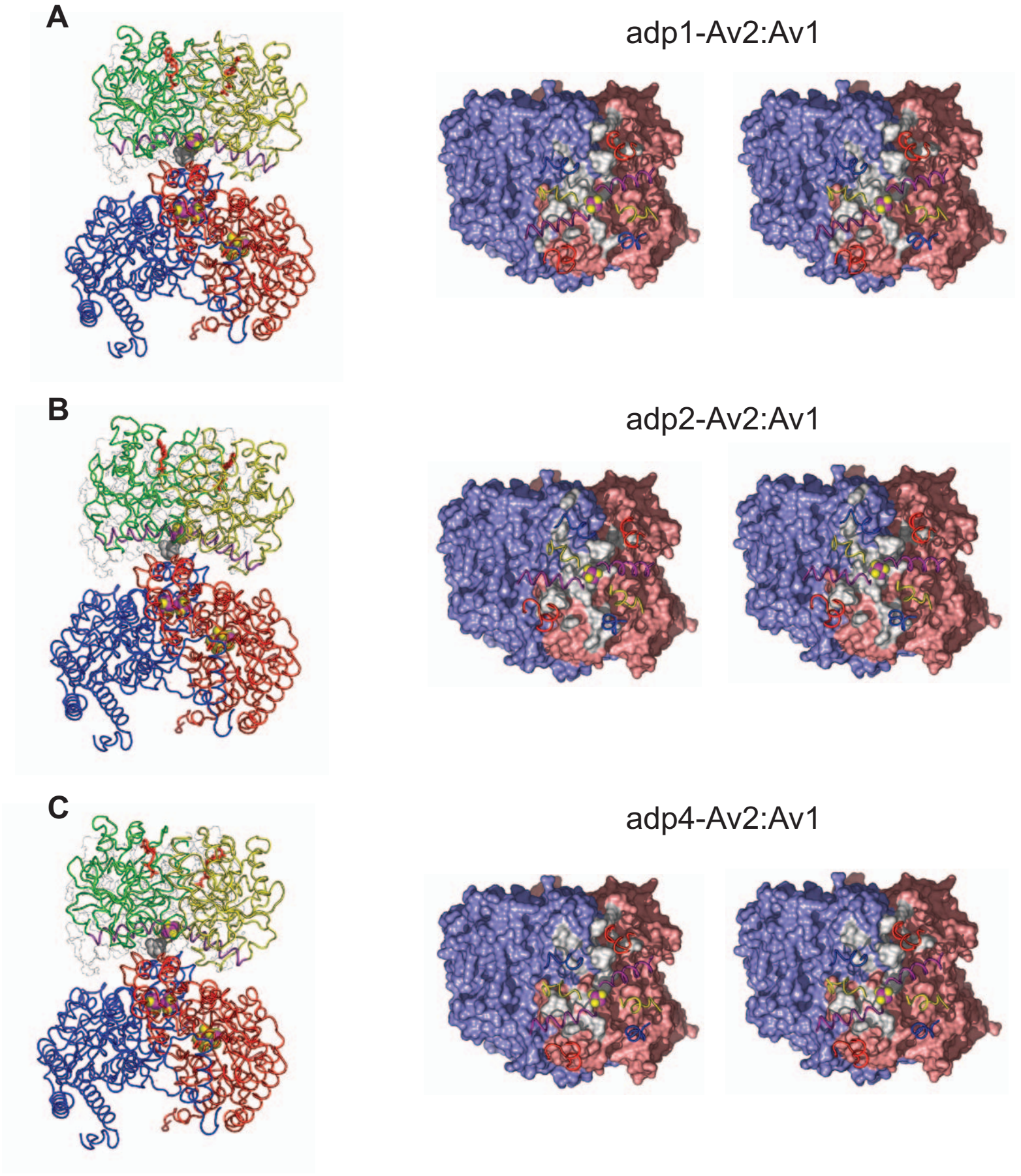

Fig. S1

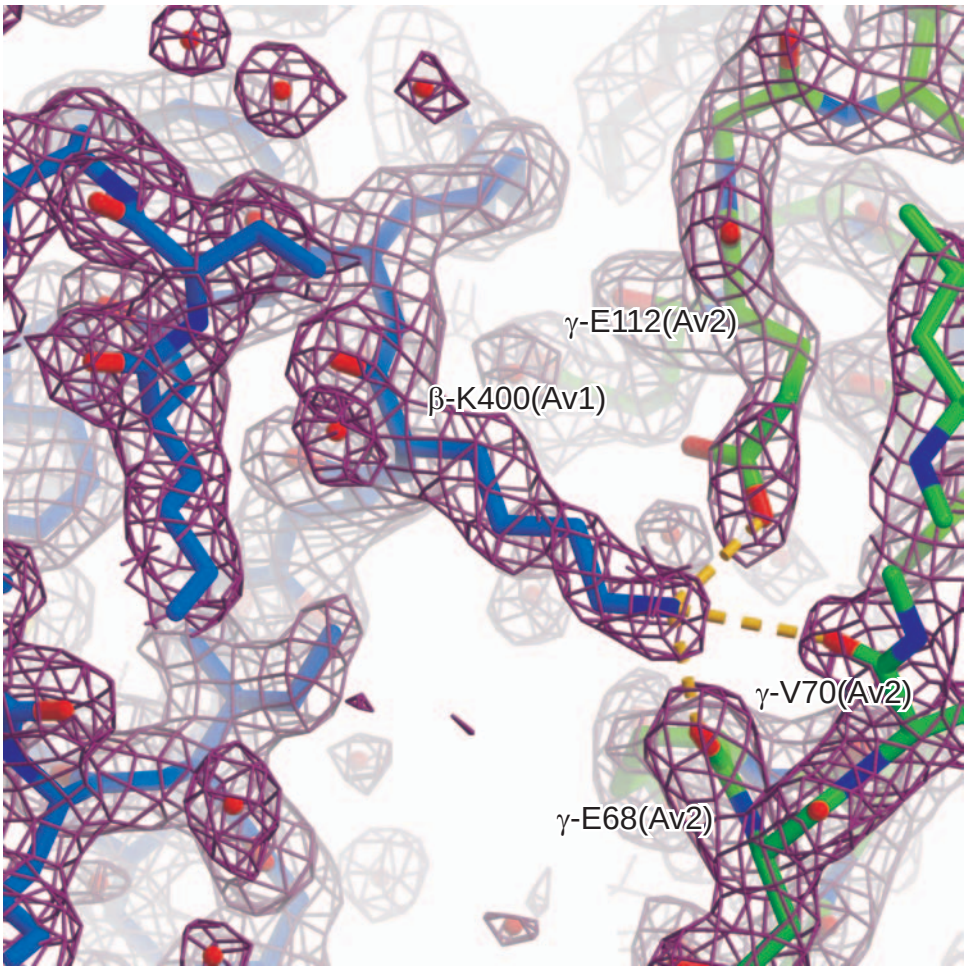

Fig. S2